



Patch loading resistance of slender plate girders with multiple longitudinal stiffeners

Balázs Kövesdi¹, László Dunai

Correspondence

Balázs Kövesdi
Budapest University of Technology and
Economics, Department of Structural
Engineering,
Műegyetem rkp. 3
1111 Budapest
Email: kovesdi.balazs@emk.bme.hu

Abstract

There is currently no reliable and simple design method available in international literature for the determination of the patch loading resistance of slender plate girders having multiple longitudinal stiffeners. Previous investigations focused mainly on girders having one longitudinal stiffener, which is not the common case for box-girder bridges. Therefore, the current research – partly published in this paper – has a focus on the patch loading resistance of slender web girders having multiple longitudinal stiffeners. An advanced numerical model is developed and verified by own laboratory test results to determine the patch loading resistance. A numerical parametric study is executed to investigate the load-carrying capacity of girders having typical bridge geometries. Analysing the numerical simulation results the structural behavior obtained is classified based on the stiffener stiffness. Effect of the different geometrical parameters on the patch loading resistance is evaluated with special focus on the stiffener stiffness and distance between the longitudinal stiffeners. The failure modes depending on the stiffener stiffness are investigated and the local buckling type failure is characterised by a minimum stiffness. For this specific failure mode an improved design method is developed for girders having multiple longitudinal stiffeners giving reliable resistance for the analysed cases within the analysed parameter range. The presented resistance model is consistent with the design philosophy of EN1993-1-5.

Keywords

patch loading, longitudinally stiffened girders, slender plate girders, multiple stiffeners, numerical simulations, design method development.

1 Introduction

In the case of slender plate girders with longitudinal stiffeners, it is known, that the patch loading resistance model of EN1993-1-5 [1] had a large scatter and it can lead to significant underestimation of the resistance. Numerous previous experimental and numerical research programs studied the patch loading resistance of longitudinally stiffened girders in order to develop a reliable resistance model. After all, there is currently no reliable and simple design method available in international literature. The main part of the previous investigations focuses on the patch loading resistance of girders having one longitudinal stiffener. In the bridge design, however, usually not only one stiffener is applied on the web, but multiple stiffeners distributed quasi-uniformly along the plate width. For these cases, the applicability of the previously developed design methods are not proved. It is also known, the design method of EN1993-1-5 [1] does not consider the location of longitudinal stiffeners properly, even having one stiffener placed on the web.

Therefore, the focus of the current paper is on the investigation of the patch loading resistance of slender web girders with multiple longitudinal stiffeners. In the current bridge design praxis, launching (Fig. 1.a) is one of the most commonly used erection method for steel bridges due to its numerous advantages. This erection method, however, introduces large local concentrated force within the web which might cause web crippling-type failure. In many cases to avoid this failure mode, additional vertical stiffeners are welded on the slender web, as shown in Fig. 1.b. However, this solution is usually extremely cost and time consuming. Numerical simulation results for existing bridge girders show, in many cases these stiffeners can be eliminated by applying a more appropriate design method for the patch loading resistance calculation for longitudinally stiffened girders. The research aim of the current study is a comprehensive investigation of the web crippling phenomena of longitudinally stiffened girders with multiple stiffeners and improvement of EN 1993-1-5 [1] based patch loading resistance model.

Within the research program all the existing experimental, analytical and numerical investigations were overviewed, evaluated and compared. Laboratory test program is designed and executed to investigate the patch loading resistance of girders with multiple longitudinal stiffeners. The test results showed the

1. Budapest University of Technology and Economics, Faculty of Civil Engineering, Department of Structural Engineering, Budapest, Hungary.

dominant failure modes and the efficiency of the longitudinal stiffeners. Based on the test results a numerical model is developed and validated to accurately determine the patch loading resistance of girders with multiple longitudinal stiffeners. A numerical parametric study is executed to investigate the load-carrying capacity of girders having typical bridge geometries. Based on a large number of numerical simulations the structural behavior is studied and the obtained failure modes are classified based on the stiffness of the stiffener. The effect of each geometrical parameter on the patch loading resistance is evaluated with special focus on the stiffness of the stiffener and distance between the longitudinal stiffeners. Finally, an improved design method is developed for girders with multiple stiffeners. The research work is completed according to the following research strategy:

- literature review in the topic of the previous investigations on the patch loading resistance,
- conducting laboratory tests on 8 large-scale test specimens to determine the patch loading resistance and analysing the dominant failure modes,
- development and validation of an advanced numerical model based on shell elements with variable geometry and different longitudinal stiffener configurations,
- numerical parametric study to investigate the observed failure modes and the effect of the different geometric parameters on the patch loading resistance,
- design method development for girders with longitudinal stiffeners.



Figure 1 Typical layout of launched box-section bridge a) launching phase; b) internal stiffeners to avoid patch loading failure

2 Literature review - previous research results

In the international literature a large number of previous investigations can be found dealing with the determination of the patch loading resistance. Main parts of these investigations are focusing on the experimental and numerical investigation of the web crippling-type failure and tries to develop more accurate analytical design equation. Within these improved design methods the effect of longitudinal stiffener is usually implemented in the critical load (F_{cr}) by improving the buckling coefficient (k_F). The reduction factor (χ_F), however, is usually determined by the same equation for stiffened and unstiffened girders. The design method of the EN1993-1-5:2006 [1] for the patch loading resistance calculation uses the analytical mechanical model of Lagerqvist and applies reduction factor developed by Graciano, Lagerqvist and Johansson [2] – [6]. Within the recent years the patch loading resistance model has been widely investigated and the reduction

factor has been statistically evaluated. Based on the extensive research work of Davaine [7], Gozzi [8] and Chacón et al. [9] the patch loading resistance model has been improved and the calculation method of the effective loading length has been enhanced. Based on the statistical evaluation of Mirambell et al. [10] a new reduction factor calculation method has been also implemented into the second generation Eurocodes, in the EN 1993-1-5 [11]. According to this improved design model the resistance can be calculated by Eq. (1) in case of patch loading “type a” according to EN1993-1-5 Figure 6.1, and this case is investigated in the current paper.

$$F_{Rd} = \chi_F \cdot \frac{l_y \cdot f_{yw} \cdot t_w}{\gamma_{M1}} \leq 1.0 \quad (1)$$

The reduction factor due to local buckling χ_F may be obtained by Eqs. (2)-(5).

$$\chi_F = \frac{1.0}{\varphi_F + \sqrt{\varphi_F^2 - \bar{\lambda}_F}} \leq 1.0 \quad (2)$$

where:

$$\varphi_F = \frac{1}{2} \left(1 + \alpha_{F0} \cdot (\bar{\lambda}_F - \bar{\lambda}_{F0}) + \bar{\lambda}_F \right) \quad (3)$$

$$\bar{\lambda}_F = \sqrt{\frac{l_y \cdot t_w \cdot f_{yw}}{F_{cr}}} \quad (4)$$

$$\alpha_{F0} = 0.75 \quad \bar{\lambda}_{F0} = 0.50 \quad \gamma_{M1} = 1.10 \quad (5)$$

The effective loaded length (l_y) is given by Eq. (6).

$$l_y = s_s + 2 \cdot t_f \cdot \left(1 + \sqrt{\frac{b_f}{t_w}} \right) \quad (6)$$

The critical load (F_{cr}) may be calculated by Eq. (7) using the buckling coefficient according to Eqs. (8)-(9) for longitudinally stiffened girders.

$$F_{cr} = 0.9 \cdot k_F \cdot E \cdot \frac{t_w^3}{h_w} \quad (7)$$

$$k_F = 6 + 2 \cdot \left(\frac{h_w}{a} \right)^2 + \left(5.44 \cdot \frac{b_1}{a} - 0.21 \right) \cdot \sqrt{\gamma_s} \quad (8)$$

$$\gamma_s = 10.9 \cdot \frac{I_{st}}{h_w \cdot t_w^3} \leq 13 \cdot \left(\frac{a}{h_w} \right)^3 + 210 \cdot \left(0.3 - \frac{b_1}{a} \right) \quad (9)$$

The used notations and the layout of the analysed girder geometries are shown in Fig. 2.

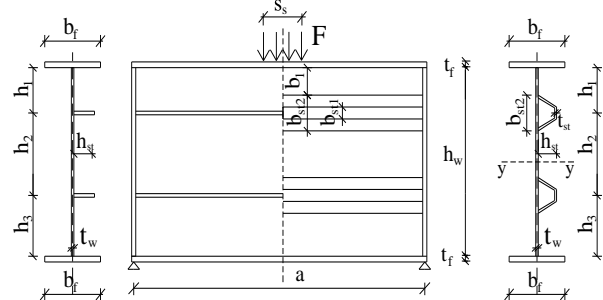


Figure 2 Used geometry and investigated structural layouts with open and closed section stiffeners.

It is well-known that the Eurocode-based design method is reliable and gives accurate patch loading resistance for unstiffened girders. However, it does not lead to accurate and reliable resistance for longitudinally stiffened girders and have relatively large scatter. Therefore, an intensive research program was completed to improve the patch loading resistance model in frame of the COMBRI-Project [12]. Within this research work Seitz [13] carried out laboratory tests and performed numerical parametric study to determine the patch loading resistance for different girder

geometries and stiffener sizes. Based on the extensive numerical study an improved design method was developed considering the interpolation between plate-like and column-like behavior of the web. The proposed design method gave accurate results for the analysed girder geometries, however it is quite complex and difficult to use in the design. Davaine [7] also executed a numerical parametric study to investigate the critical load and the ultimate resistance of longitudinally stiffened girders. Based on her investigations it was found that the main reason of the difference within the analytical and numerical results comes from the fact, that the web crippling-type failure can happen in the upper or in the lower sub-panel and the design method does not follow the correct trend for both cases. Therefore, an enhanced design method was developed considering the failure mode of the different sub-panels (failure in the upper or lower sub-panel). This design equation follows the trend of the numerical simulations and gives much closer resistance to the numerically calculated values. However, this design equation is developed for girders with one stiffener, and it cannot be applied for multiple stiffened girders. Graciano and Lagerqvist also studied in 2003 the critical buckling load related to patch loading for longitudinally stiffened girders [14]. The research was continued by Graciano and Mendes in 2014 [15]. Based on their extensive investigations the relevant values of the buckling coefficient (k_F) were determined for all investigated girder geometries, and a design equation was developed to determine the buckling coefficient (k_F). However, further studies of Graciano [16] pointed out that the above mentioned design methods should be improved. It has been found the best design equation for the patch loading resistance calculation can result in 20-60% difference (underestimation) compared to the measured or numerically simulated resistances. Therefore, the improvement of the patch loading resistance model is still an important task within the design of longitudinally stiffened girders. Based on the literature review it can be also concluded, that all the previous researchers were mainly focusing on stiffened girders having one longitudinally stiffener and no significant investigation can be found on girders having multiple longitudinal stiffeners, which is the topic of the current paper. Therefore, the present study is a unique analysis and gives new aspects to the design of box-section steel bridges.

3 Experimental investigations

An experimental research program has been conducted at the Budapest University of Technology and Economics, Department of Structural Engineering between 2015-2016. These laboratory tests are used as background for the numerical model verification and validation and gave intention on the stability failure mode characterisation and prove of the expected structural behavior of the longitudinal stiffeners. Within the laboratory test program 8 specimens (4 different configurations) are investigated.

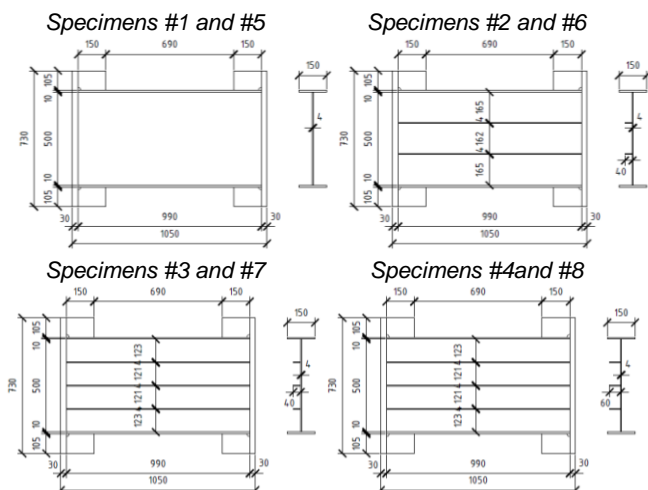


Figure 3 Geometry of the test specimens.

Two girders had no stiffener (unstiffened - reference specimens) and six specimens had 2 or 3 longitudinal stiffeners placed on the web. For each specimens the longitudinal stiffeners were uniformly distributed along the girder depth. The geometry of the specimens can be seen in Fig. 3, the measured load displacement curves are presented in Figs. 4-5.

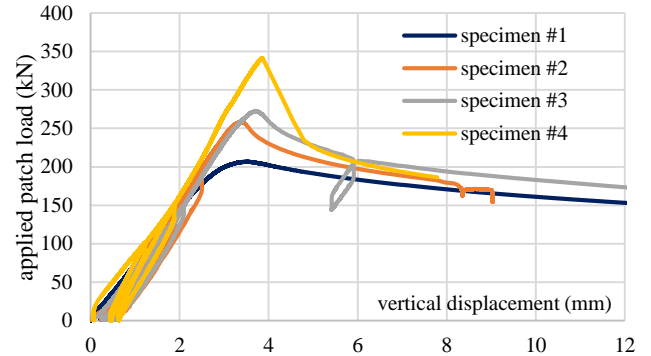


Figure 4 Load displacement curve of specimens #1 – 4

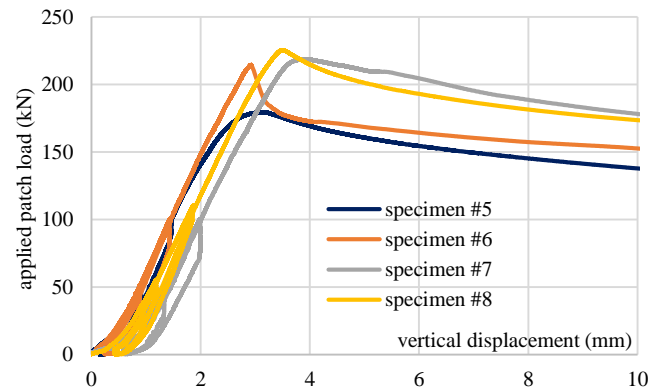


Figure 5 Load displacement curve of specimens #5 – 8

All specimens were manufactured with a web plate of 500x4 mm, and flange plates of 150x10 mm. The length of the specimens was constant, 1050 mm. The stiffener size and numbers were varied within the test program. Two stiffener sizes are applied 40x4 mm and 60x4 mm plate plate stiffeners. Table 1 summarizes the applied stiffener number and sizes and also gives the measured resistances ($F_{R,test}$). Thus the material properties of the different web plates had differences, the measured resistances are adjusted based on the material test results to bring them comparable. The adjusted resistances are also noted by $F_{R,test,mod}$ in Table 1. The adjusted resistances show the differences coming from the structural layout and/or imperfections of the specimens.

Table 1 Test specimens and patch loading resistances

specimen	stiffener number	stiffener size	γ_s	s_s [mm]	$F_{R,test}$ [kN]	$F_{R,test,mod}$ [kN]	$F_{R,num}$ [kN]
#1	0	-	0	200	206.4	224.6	204.6
#2	2	40-4	27.27	200	258.4	252.9	254.8
#3	3	40-4	27.27	200	270.9	271.2	266.8
#4	3	60-4	80.55	200	320.4	317.6	268.2
#5	0	-	0	100	180.2	182.1	176.5
#6	2	40-4	27.27	100	214.3	194.5	207.9
#7	3	40-4	27.27	100	218.4	227.4	191.6
#8	3	60-4	80.55	100	223.8	223.9	208.9

The typical failure mode of the test specimens is shown in Fig. 6, which is always the local web crippling of the sub-panels between the loaded flange and the upper longitudinal stiffener. The test program has been separately published with all the details in [17]. The main conclusions of the test results were that relatively small stiffeners are strong enough to localize the failure mode within the web sub-panel and to eliminate global buckling of the entire web. This observation gave the intention for the practical design situations the separation of the failure modes (local and global) could be efficient and it could be made based on the relative stiffness of the stiffeners. Since the test results proved relatively weak stiffeners can be effective to eliminate global buckling, the further focus of the research program is put on the local buckling resistance calculation of the web sub-panels under patch load.



Figure 6 Typical obtained failure mode of test specimens

4 Numerical investigations

4.1 Development of the numerical model

The developed numerical model applied for the patch loading resistance calculation is shown in Fig. 7 for two test specimens. It is a full shell model using four node thin shell elements. The numerical model is developed in Ansys [18]. The two end plates are pinned supported along the lower edges and laterally supported to eliminate the rotation of the end cross-sections. The transverse load is applied in the middle of the test specimens. To consider the load introduction plate (which had a large stiffness compared to the upper flange), the rotational DOFs are coupled at the load introduction length at the location of the patch load. All the applied support and load condition refers to the laboratory test layout.

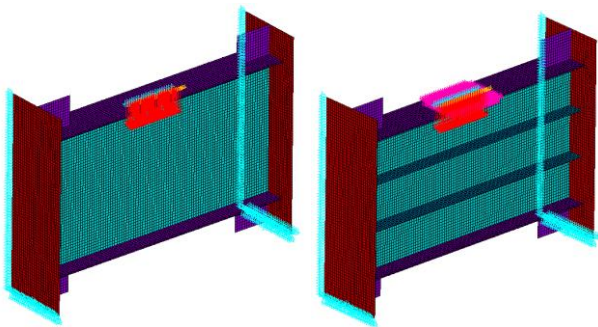


Figure 7 Numerical model of test specimens

The numerical model is used for the determination of the critical (F_{cr}) and ultimate load (F_{ult}) of the analysed girders. The critical load is determined using linear buckling analysis (LBA). The ultimate load is determined by geometric and material nonlinear analysis using equivalent geometric imperfections (GMNIA).

4.2 Material model and imperfections

Thus the applied imperfections are highly important for the patch

loading resistance calculation as proved by Kövesdi et al. [17], a detailed imperfection sensitivity analysis is executed before the numerical parametric study. The analysed imperfections shapes for a specimen having one longitudinal stiffener are presented in Fig. 8. Similar study has been executed for girders having 2 and 3 longitudinal stiffeners on the web.

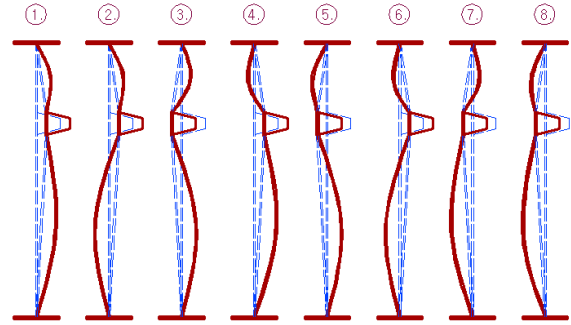


Figure 8 Analysed imperfection shapes

Global and local imperfection shapes are both considered with an amplitude of $h_w/200$ for the global, and $b/200$ for the local buckling, where h_w is the entire web depth, b is the depth of the web sub-panels. The most detrimental imperfection layout is selected for the determination of the patch loading resistance and it was used in the further numerical parametric study. More details on the imperfection sensitivity analysis can be found in [17].

In the presented research program two material models are applied. The first one is used to the model validation and the second one to the numerical parametric study. In both models linear elastic – hardening plastic material model with von Mises yield criterion is used applying isotropic hardening rule in the plastic domain. The material is assumed to behave linearly elastic and to obey Hooke's law with a Young's modulus equal to 210000 MPa up to the yield stress. Thereafter and until it reaches the ultimate stress, the material is assumed to behave linearly with a hardening modulus. The ultimate strength is defined by $\epsilon=12\%$, which fits to the average material tests.

4.3 Model verification and validation

At first the numerical model is verified and validated. Results of the numerical model verification is shown in Fig. 9. Based on the conducted mesh sensitivity analysis all the web sub-panels are divided at least into 10 finite elements leading to appropriate resistance.

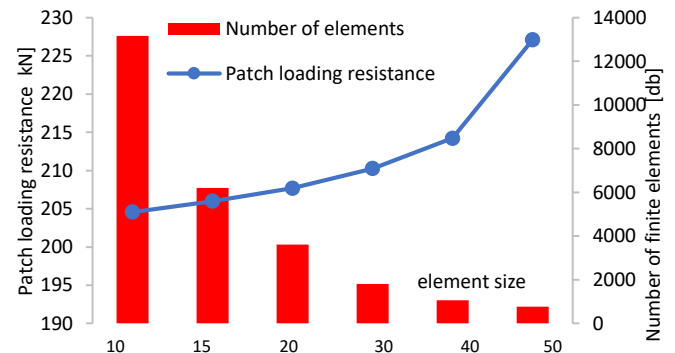


Figure 9 Results of the model verification

The model validation is executed at first (i) by the comparison of the numerical results to the test-based measured resistances and (ii) by the comparison of the computed and measured failure modes. Results show, the developed numerical model is highly accurate. The calculated resistances are summarized in Table 1 for all test specimens and the comparison of the failure modes are

presented for one case in Fig. 10.

Results prove the developed numerical model gives safe side resistances with the applied most detrimental imperfection configurations in case of all test specimens. Therefore, based on the verification and validation of the numerical model the accuracy of the model is proved and considered to be appropriate for further numerical parametric study.

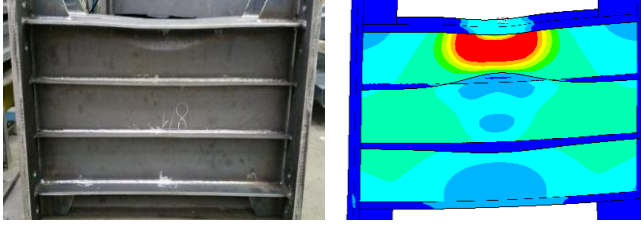


Figure 10 Results of the model verification

4.4 Results of the numerical parametric study

An extensive numerical parametric study is executed to analyse the patch loading failure mode and to identify the trends of the different geometric parameters on the structural behavior and resistance. The numerical parametric study had two separated parts but referring to the same geometrical configurations:

- (i) investigation of the critical load (F_{cr}),
- (ii) investigation of the patch loading resistance (F_{ult}).

A total of 2500 different girder geometries are investigated and for all geometrical configurations the buckling load (F_{cr}) and the patch loading resistance (F_{ult}) are determined. Within the parametric study the parameters listed in Table 2 are varied within the given parameter ranges. All notations are given in Fig. 2. By changing the geometrical parameters the following characteristic parameter ratio ranges are investigated: $b_1/h_w = 0.15 - 0.45$, $h_w/t_w = 80 - 500$, $b_1/t_w = 25 - 167$ and $s_s/a = 0.2 - 0.8$, which parameter ranges refers the typical geometries used for bridges.

Table 2 Varied parameters and studied parameter ranges.

	a [mm]	h_w [mm]	t_w [mm]	b_f [mm]	t_f [mm]	s_s [mm]
Min.	2400	1200	3	260	12	200
Max.	6000	4000	20	600	40	2000
	b_1 [mm]	h_{st} [mm]	t_{st} [mm]	γ_s	b_1/h_w	b_1/t_w
Min.	250	80	4	60	0.15	25
Max.	1000	290	20	4600	0.45	167

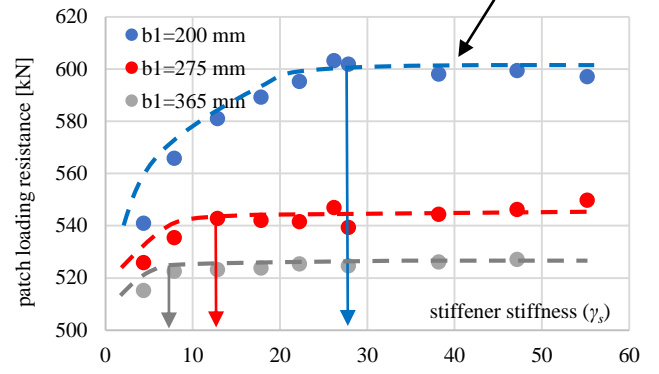
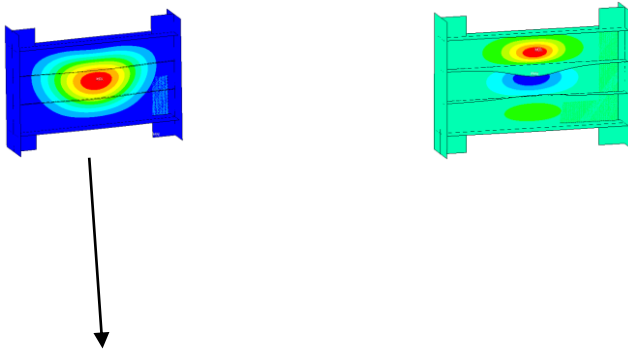


Figure 11 Effect of stiffener stiffness on patch loading resistance

Within the numerical parametric study it was investigated first, how the stiffener stiffness (γ_s) does influence the patch loading resistance. Some of the obtained results are presented in Fig. 11. All the numerical calculations show similar trends. If weak stiffeners are applied on the web, or no stiffeners are used, the failure mode is global buckling of the entire web panel. By increasing the stiffener stiffness the patch loading resistance increases until the global buckling failure mode turns into local buckling, where further increase in the stiffener size does not effect the resistance, as shown in Fig. 11. The patch loading resistance values show a clear trend which has an increasing part and a quasi-constant domain. The intersection point between these two different structural behavior can be determined and used as a characteristic measure for the separation of the global and local failure modes.

Within the numerical parametric study the minimum stiffener stiffness is determined for all analysed girder geometries, which can ensure local buckling-type failure mode within the sub-panel of the web. The calculation results show, all these minimum stiffness values were smaller (sometimes significantly smaller) than the maximum stiffener stiffness given by Eq. (10) to be allowed to consider in the critical buckling load according to EN 1993-1-5 [1].

It is also found this limit value returns usually smaller stiffener stiffness values, which are used in the bridge design praxis. It means, the main part of the real practical cases are designed using so called "strong" stiffeners, which are able to localise the buckling failure within the sub-panel. Therefore, within the further studies only girders having "strong" stiffeners are investigated and the obtained results and tendencies are valid for the local buckling-type failure mode where strong stiffeners ensure the separation of the buckling shapes within the web sub-panels.

$$\gamma_{s, \lim} \leq 13 \cdot \left(\frac{a}{h_w} \right)^3 + 210 \cdot \left(0.3 - \frac{b_1}{a} \right) \quad (10)$$

$$\text{where } \gamma_s = 10.9 \cdot \frac{I_{st}}{h_w \cdot t_w^3} \quad (11)$$

The effect of the main geometrical parameters on the critical buckling load are determined separately and evaluated on graphs. The main parameters having influence on the critical buckling load and their trends are shown by Figs. 12-14. The horizontal axis of each graph shows the analysed geometrical parameter and the vertical axis show the value of the critical buckling load.

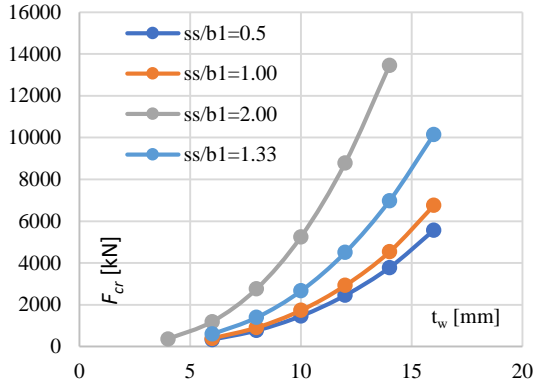


Figure 12 Effect of stiffener stiffness on patch loading resistance

Results prove, the critical buckling load increases by increasing the thickness of the web (t_w), by decreasing the sub-panel depth (b_1) and the load introduction length (s_s). There is a clear trend shown in Fig. 13 between b_1/t_w^3 ratio and the critical buckling load. The same trend can be obtained for various s_s/b_1 ratios making the entire evaluation process dimensionless.

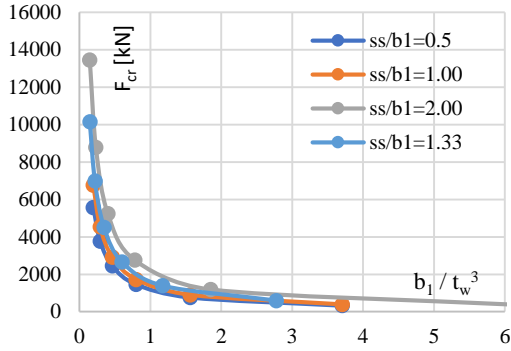


Figure 13 Effect of stiffener stiffness on patch loading resistance

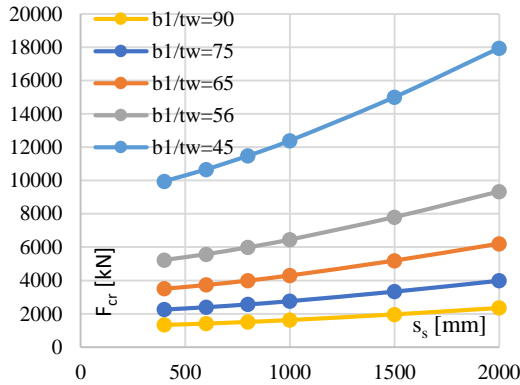


Figure 14 Effect of stiffener stiffness on patch loading resistance

Further studies show there are another parameters, which might slightly influence the patch loading resistance and the critical buckling load. For example increase in the flange size (b_f , t_f) can cause increase in the critical buckling load, however, this effect is marginal compared to the previously presented parameters. The trend for each parameter are determined on the way, that only one parameter has been changed within the study to be able to clearly separate the effect of each parameter independently.

5 The developed enhanced analytical model

Based on the results of the numerical parametric study the calculation method of the critical buckling load and the reduction factor for the ultimate load calculation are evaluated and enhanced

design equations are proposed for both. The numerical results prove the critical buckling load should be calculated for the analysed failure mode based on the b_1/t_w^3 ratio instead of the h_w/t_w^3 ratio, therefore the original design equation of the EN 1993-1-5 [11] has been changed to Eq. (12). Within this equation all the other terms are kept unchanged, only this ratio is modified.

$$F_{cr} = 0.9 \cdot k_F \cdot E \cdot \frac{t_w^3}{b_1} \quad (12)$$

From the numerically calculated buckling load using Eq. (12) the required values of the k_F buckling coefficient are back-calculated. It is proved, the mostly dominant parameter within the buckling coefficient is the s_s/b_1 ratio, which trend is shown in Fig. 15 for geometries using closed section longitudinal stiffeners.

Further evaluation proved, the buckling coefficient slightly depends on the b_1/t_w and $((b_f \cdot t_f^3)/(b_1 \cdot t_w^3))$ ratios as well. The most accurate equation for the buckling coefficient is given by Eq. (13), in which the first two terms governs the calculation. The red line shown in Fig. 15 presents the design equation containing only the first two terms, where the results only depend on the b_1/t_w ratio.

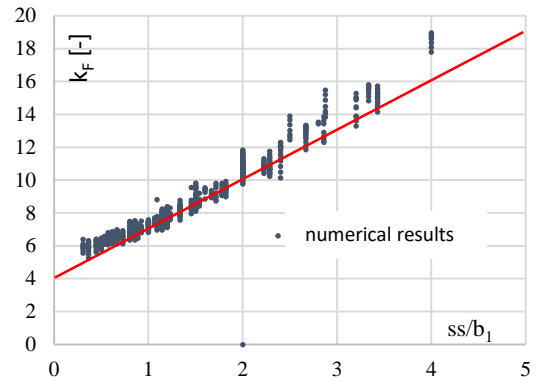


Figure 15 Effect of s_s/b_1 ratio on the buckling coefficient

$$k_F = 4.0 + 3.0 \cdot \frac{s_s}{b_1} - 0.01 \cdot \frac{b_1}{t_w} + 0.2 \cdot \sqrt[4]{\frac{b_f \cdot t_f^3}{b_1 \cdot t_w^3}} \quad (13)$$

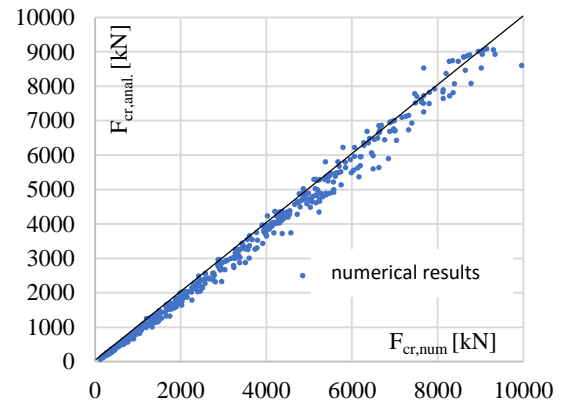


Figure 16 Comparison of numerically and analytically calculated buckling load

Comparison of the analytically and numerically calculated buckling loads are given in Fig. 16, where the analytical solution uses Eq. (12)-(13) for the critical load and buckling coefficient calculation, respectively. For the entire database the average and the maximum difference is 4,3% and 17,3%, respectively, with a standard deviation equal to 0,05.

The numerical calculations prove, the closed section stiffeners coming from its torsional rigidity provides larger buckling coefficients for the web. Similar numerical study as presented above is also executed for girders having open section flate plate longitudinal stiffeners. The results show the same geometric

parameters have influence on the patch loading resistance and critical buckling load values, however, the buckling coefficient is smaller coming from the smaller torsional rigidity and its accurate value might be calculated by Eq. (14). This equation is similar to the first two terms of Eq. (13) just changing the constant from 3.0 to 1.5.

$$k_F = 4.0 + 1.5 \cdot \frac{s_s}{b_1} \quad (14)$$

The comparison of the analytical results to the numerically computed values show the average difference of 1.9% with a standard deviation equal to 0.1.

Using the improved buckling load, the relative slenderness of all the analysed girders are calculated and the necessary reduction factors are back-calculated from Eq. (1) using the effective loaded length determined by Eq. (6). Results are presented in Fig. 17. The horizontal axis shows the relative slenderness ratio according to Eq. (4) using the analytically calculated critical load (F_{cr}). The vertical axis shows the back-calculated reduction factors (χ_F).

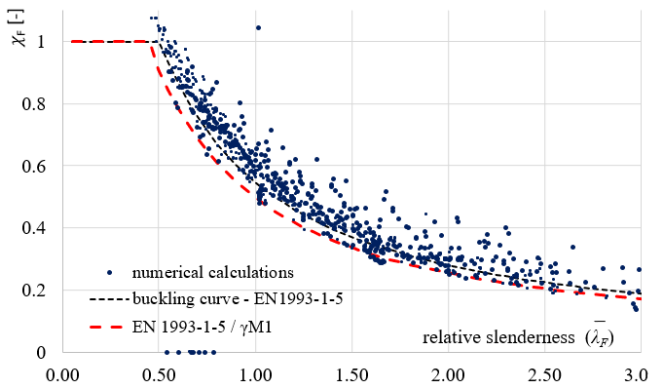


Figure 17 Back-calculated reduction factors for the patch loading resistance

Results prove the analytical solution using the improved buckling load and the currently proposed effective loaded length calculation method and the buckling curve related to patch loading resistance gives safe side resistances. The red dashed line presenting the design value of the reduction factor gives lower bound curve for all the 2500 numerical simulation results. It proves, the current design method of the EN 1993-1-5 would give safe side resistances using the improved and more accurate buckling loads as well.

However, results also show, there is a large scatter in the obtained resistance values and therefore, a more appropriate calculation method is developed. Considering Eqs. (15)-(16) it can be observed, the relative slenderness and also the back-calculated reduction factor also depend on the effective loaded length (l_y). All the other parameters of the calculation process are geometrical (t_w) or material (f_y) constants.

$$\bar{\lambda}_F = \sqrt{\frac{l_y \cdot t_w \cdot f_{yw}}{F_{cr}}} \quad (15)$$

$$F_{Rd} = \chi_F \cdot \frac{l_y \cdot f_{yw} \cdot t_w}{\gamma_{M1}} \leq 1.0 \quad (16)$$

Therefore, the accurate values of the effective loaded length are back-calculated from the numerical calculation results and the main dominant parameters, which have influence on its value are determined. The value of the effective loaded length has two terms. At first the loading length (s_s) has a physical meaning and its value can be considered as a given constant parameter for all analysed cases. Therefore, its effect has been separated and the equation of l_y is modified according to Eq. (17). The accurate value of the

second term (l_{add}) is determined to each analysed geometry and evaluated in a detailed manner. The second term of Eq. (17) should have a physical meaning and its value should depend on the analysed girder geometry, especially on the size of the loaded flange and the web sub-panel b_1/t_w ratio.

$$l_y = s_s + 2 \cdot t_f \cdot \left(1 + \sqrt{\frac{b_f}{t_w}} \right) = s_s + l_{add} \quad (17)$$

Results show the main parameters which have influence on the effective loaded length are the loading length (s_s) and the b_1/t_w and t_f/t_w ratios. The determined trends are shown in Figs. 18-19.

Diagram shows the effective loaded length increases, if the b_1/t_w ratio of the web plate increases and it decreases, if the t_f/t_w ratio increases. The physical meaning of these results is if the web plate is more weak compared to the flange, the flange can better distribute the concentrated force along the web, and the patch load can result in a more uniform stress distribution which can lead to larger effective loaded length.

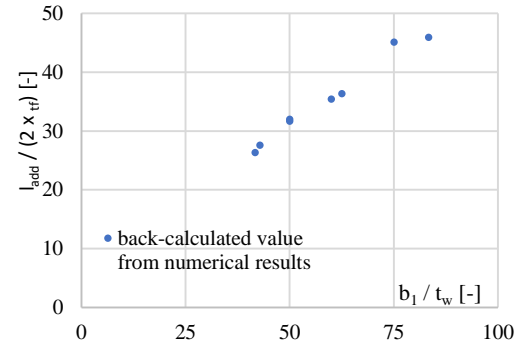


Figure 18 Back-calculated value of the effective loaded length depending on the b_1/t_w ratio

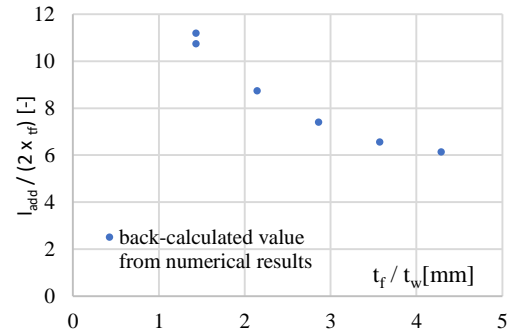


Figure 19 Back-calculated value of the effective loaded length depending on the t_f/t_w ratio

Based on the numerical results an improved equation is developed for the more accurate determination of the effective loaded length given by Eq. (18).

$$l_y = \begin{cases} s_s + 2 \cdot t_f \cdot \left[\sqrt{\frac{t_w}{t_f}} \cdot \left(0.5 \cdot \frac{b_1}{t_w} - 10 \right) \right] & \text{ha } 20 < \frac{b_1}{t_w} \leq 70 \\ s_s + 2 \cdot t_f \cdot \left[\sqrt{\frac{t_w}{t_f}} \cdot 0.2 \cdot \frac{b_1}{t_w} \cdot \frac{b_1}{s_s} \right] & \text{ha } \frac{b_1}{t_w} > 70 \end{cases} \quad (18)$$

The effective loaded length has also a physical meaning, that it can adjust the value of the numerically calculated datapoints presented in Fig. 17 not only along the vertical but also along the horizontal axis. It means, by an accurate determination of the effective loaded length the scatter obtained in the numerical simulation results can be significantly reduced. Figure 20 shows the back-calculated reduction factors using the improved equation for the effective

loaded length.

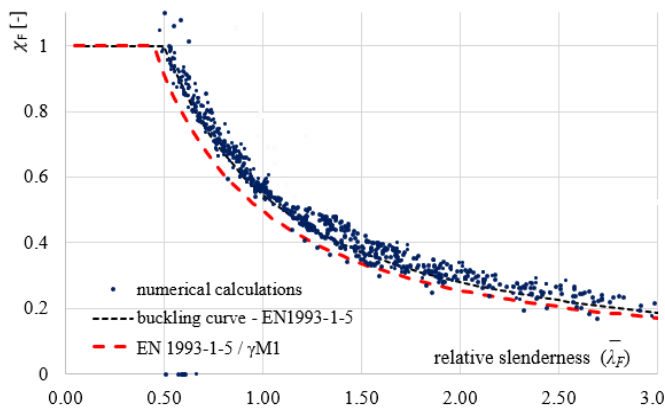


Figure 20 Back-calculated reduction factors for the patch loading resistance using improved buckling load and effective loaded length

Results prove the scatter has been significantly reduced and all the calculation results are still on the safe side using the patch loading-type buckling curve of the EN 1993-1-5 [11] using partial safety factor equal to $\gamma_{M1}=1.1$. The average ratio of the analytical and numerical results has been changed to 0.91 with a standard deviation of 0.07, which values prove the accuracy of the new improved design equation to determine the patch loading resistance of girders with multiple longitudinal stiffeners.

6 Conclusions

The present paper introduces an improved design method for the patch loading resistance of multiple stiffened girders. An extensive research program is carried out to determine the accurate value of the patch loading resistance. The executed research consists of laboratory experiments, extensive numerical investigations and development of analytical design equations. The new findings based on the research results are the followings:

- it has been shown, the failure modes can be separated between local and global buckling based on the stiffness criterion of the longitudinal stiffeners,
- minimum stiffness criteria is determined to identify the local buckling failure within the loaded sub-panel of the web,
- design equation is developed for the critical buckling load calculation for the local buckling-type failure mode,
- improved design equation is developed for the novel calculation of the effective loaded length,
- it has been proved that using the improved design equations for the critical buckling load and the effective loaded length, the buckling curve of EN 1993-1-5 can be used with adequate safety to determine the patch loading resistance.

Acknowledgement

The presented research program has been financially supported by the Grant MTA-BME Lendület LP2021-06 / 2021 "Theory of new generation steel bridges" program of the Hungarian Academy of Sciences, which is gratefully acknowledged.

References

- [1] EN1993-1-5:2005, Eurocode3: Design of steel structures, Part 1-5: Plated Structural elements, 2006.
- [2] Lagerqvist, O. (1995) Patch loading resistance of steel girders subjected to concentrated forces, Doctoral thesis, 1994:159D, Luleå University of Technology, Division of Steel Structures, Luleå, Sweden.
- [3] Lagerqvist, O.; Johansson, B. (1996) Resistance of I-girders to concentrated loads, *Journal of Constructional Steel*

- Research. 39(2), 87-119.
- [4] Graciano, C.A. (2002) Patch loading – Resistance of longitudinally stiffened steel girder webs. PhD thesis, 2002:18, Luleå University of Technology. Division of Steel Structures, Luleå, Sweden.
- [5] Graciano, C.; Johansson B. (2003) Resistance of longitudinally stiffened I-girders subjected to concentrated loads, *Journal of Constructional Steel Research*. 59(5), 561-586.
- [6] Graciano, C. (2005) Strength of longitudinally stiffened webs subjected to concentrated loading, *J.Struct.Eng.ASCE*. 131(2), 268-278.
- [7] Davaine, L. (2005) Formulation de la résistance au lancement d'une âme métallique de pont raidie longitudinalement, Doctoral thesis D05-05, INSA de Rennes, France, 2005 (in French).
- [8] Gozzi, J. (2007) Patch loading resistance of plated girders. Doctoral thesis 2007:30, Luleå University of Technology, Sweden. ISRN: LTU-DT-07/30--SE.
- [9] Chacón, R.; Mirambell, E.; Real, E. (2010) Hybrid steel plate girders subjected to patch loading, Part 2: Design proposal, *Journal of Constructional Steel Research*. 66(5), 709-715.
- [10] Mirambell, E.; Chacón, R.; Kuhlmann, U.; Braun, B. (2021) Statistical evaluation of the new resistance model for steel plate girders subjected to patch loading, *Steel Construction*. 1(5), 10-15.
- [11] EN1993-1-5:2024, Eurocode3: Design of steel structures, Part 1-5: Plated Structural elements (before publication).
- [12] COMBRI: Competitive Steel and Composite Bridges by Improved Steel Plated Structures. Final Report, RFCS Research Project RFS-CR-03018, 2007.
- [13] Seitz, M. (2005) Tragverhalten längsversteifter Blechträger unter quergerichteter Krafteinleitung. Doctoral thesis, Universität Stuttgart, Mitteilung des Instituts für Konstruktion und Entwurf Nr.2005-2 (in German).
- [14] Graciano, C.; Lagerqvist, O. (2003) Critical buckling of longitudinally stiffened webs subjected to compressive edge loads, *Journal of Constructional Steel Research*. 59(9), 1119-1146.
- [15] Graciano, C.; Mendes, J. (2014) Elastic buckling of longitudinally stiffened patch loaded plate girders using factorial design, *Journal of Constructional Steel Research*. 100, 229-236.
- [16] Graciano, C. (2015) Patch loading resistance of longitudinally stiffened girders – A systematic review, *Thin-Walled Structures*. 95, 1-6.
- [17] Kövesdi, B.; Mecséri, B.J.; Dunai, L. (2018) "Imperfection analysis on the patch loading resistance of girders with open section longitudinal stiffeners", *Thin-Walled Structures*, 123, 195-205.
- [18] ANSYS® v16.5, Canonsburg, Pennsylvania, USA.